

## OPEN ACCESS

*This is an open access article distributed under the terms of the Creative Commons Attribution License, which permits unrestricted use, distribution, and reproduction in any medium, provided the original author and source are credited.*

<sup>1</sup>Basrah Engineering Technical College, Southern Technical University, Basrah, Iraq

<sup>2</sup>Department of Computer Engineering, University of Basrah, Basrah, Iraq

Correspondence to:  
Issa Ahmed Abed,  
issaahmedabed@stu.edu.iq

Additional material is published online only. To view please visit the journal online.

Cite this as: Alraouf DAAA, Abed IA and Al-Ibadi A. Proposed Design for Pneumatic Artificial Muscles in Soft Robotics System: An Experimental Study. Premier Journal of Science 2025;15:100178

DOI: <https://doi.org/10.70389/PJS.100178>

Peer Review

Received: 14 August 2025

Last revised: 31 October 2025

Accepted: 1 November 2025

Version accepted: 4

Published: 12 December 2025

Ethical approval: N/a

Consent: N/a

Funding: No industry funding

Conflicts of interest: N/a

Author contribution:

Duha Abd Alameer Abd Alraouf, Issa Ahmed Abed and Alaa Al-Ibadi –  
Conceptualization, Writing – original draft, review and editing

# Proposed Design for Pneumatic Artificial Muscles in Soft Robotics System: An Experimental Study

Duha Abd Alameer Abd Alraouf<sup>1</sup>, Issa Ahmed Abed<sup>1</sup>  and Alaa Al-Ibadi<sup>2</sup>

## ABSTRACT

The artificial pneumatic muscle is considered one of the essential flexible actuators used in soft robotics due to its advantages, which include flexibility, light-weight, efficiency, and high tensile strength compared to weight. However, despite these advantages, there is a nonlinear behavior that appears known as hysteresis, which shows a clear difference between the response when increasing and decreasing pressure, which complicates the control process and affects its accuracy. In this research, an experimental study was conducted to examine the hysteresis phenomenon by measuring the relationship between pressure and muscle length in the two stages of increasing and decreasing pressure. By employing experimental data and adopting the arc tangent function, hysteresis was accurately modelled. After that, the results showed an excellent agreement between the mathematical model and the experimental data by found Statistical evaluation for model, which confirms the effectiveness of the function in embodying this nonlinear performance. This model provides a means to develop the control of artificial pneumatic muscle and can be used with different sizes of air muscles made of the same materials because it is pressure dependent, which contributes to the development of applications based on prosthetic limbs and soft robotics.

**Keywords:** Pneumatic artificial muscle actuator, Hysteresis characterization, Arc tangent hysteresis model, Pressure–length relationship, Nonlinear least-squares fitting

## Introduction

Possible future uses for robotic systems include exoskeletons worn to restore or enhance human skills, personal or mobile robots that work alongside people, and a general uptick in robotics research and development. Because they are pliable and gentle, Pneumatic artificial muscles (PAMs) have emerged as an alternative to other actuators on the market over the last 30 years due to their gentle nature and ability to actuate. Researchers in the domain of artificial muscle actuators come from a wide variety of academic backgrounds, including physics, biology, mechanical engineering, materials science, and electrical engineering. PAMs are simple mechanical actuators that have an elastomeric bladder enclosed in a braided mesh sleeve that is sealed at both ends by two end-fittings.

When air is pumped into the bladder, the actuator may either shorten or lengthen along the axis, depending on which way the braided sleeve fibres are twisted. Contractile PAMs, sometimes called contractile

actuators, are more popular than extensile PAMs because they can generate stronger forces with less chance of buckling.

Electric motors, hydraulic actuators, pneumatic pistons, shape memory alloys (SMA), and flexible actuators are a few examples of traditional actuation methods.<sup>1</sup> The following are some of the main reasons why artificial muscles are preferable to alternative actuation mechanisms<sup>2</sup> include low weight, quick responsiveness, simple installation, excellent power-to-weight ratio, minimal production cost, great dexterity and safety, big deformations<sup>3</sup> structural pliability don't have mechanical wear since it lacks internal moving parts, in addition to its clean operation.<sup>4</sup> Despite these features the nonlinear hysteretic nature of PAMs makes tracking control of PAM-driven robots problematic the friction between the sheath threads and the material characteristics of the silicone tube cause this performance.<sup>5,6</sup> Hence, PAM hysteresis modelling has received a lot of attention. The hysteresis characterization of PAMs is described using many models loosely grouped into two groups: operator-based models and differential-based models. The Duhem model, Bouc-Wen model, and variants thereof are all members of the first family. These models are defined by a system of nonlinear differential equations that describe hysteresis loop form. It is problematic for feed-forward because, although the differential-based model can account for the impact of PMA's velocity, it is difficult to determine its inversion and compensate for hysteresis. In order to address this issue, many operator-based models were examined,<sup>7</sup> including the Preisach model, the classical Prandtl-Ishlinskii (CPI) model, and verifications of it. In most cases, these models use many operators to characterize the hysteresis.<sup>8</sup> Below are some studies regarding hysteresis; Ru et al. (2024) presented a study to treat hysteresis in pneumatic actuators using a modified Prandtl-Ishlinskii model with prediction algorithms and fuzzy neural networks. The model was proven correct by practical experiments by developing motion control. However, it is necessary to take into account complex calculations and test it on other actuators.<sup>9</sup> Sofa et al. (2021) developed a modified model of the Bouc-wen model that represents the hysteresis in aerobic muscles. The model focused on the relationship between muscle length and force output, which supported the accuracy of describing hysteresis loops, in addition to providing a model that describes the effect of pressure on force. The model was experimentally validated with muscles of different lengths. This work is considered a good step in enhancing the control systems of soft robots that use aerobic muscles.

Guarantor: Issa Ahmed Abed

Provenance and peer-review:  
Unsolicited and externally peer-reviewed

Data availability statement:  
All the data is provided in the manuscript

The results prove that the model provides better performance than the traditional model in describing the dynamic performance of muscles.<sup>10</sup> Shakiba et al. (2021) proposed a solution to the hysteretic behaviour of artificial muscles by means of a feed-forward controller based on the velocity-based Prandtl-Ishlinskii model. A direct inverse model based on the GPI model was used to extract the parameters instead of the complex calculations of the inverse model. The model was enhanced by a genetic algorithm and interior point methods to determine the parameters accurately and quickly. The method proved to be able to compensate for hysteresis effectively by experiment and is therefore suitable for high-frequency motion applications. Ru et al. (2023) researchers presented an improved rate-dependent modified generalized Prandtl-Ishlinskii (RMGPI) model to describe the complex hysteresis in pneumatic actuators made of silicone rubber. The rate-based and asymmetric hysteresis were considered, and the actual bending angle was then determined using an optical feedback system. To address the problem of setting model parameters with many operations. So, to improve the definition efficiency, they developed an evolutionary firefly algorithm. Studies and experiments have proven the effectiveness of the model and the proposed algorithm.<sup>11</sup> Ma et al. (2024) proposed a new mechanical model to improve the accuracy of describing hysteresis in pneumatic muscles during elbow joint movement using aerobic muscles. To support the accuracy of representing movement and resistance in the system, the model included a velocity-force relationship that resembles the movement of skeletal muscles;<sup>12</sup> Shang et al. (2024) presented a complete model for predicting the continuous and stiffness-coupled hysteresis of a soft actuator driven by artificial antenna muscles. The researchers used a fuzzy neural network targeting the analysis of internal hysteresis, actuator coupling, and hysteresis. An effective inverse compensator was developed to decouple and reduce the hysteresis in the system. A significant improvement in the orientation and hysteresis reduction was demonstrated through the experiments, which achieved the effectiveness of the model. The results showed that the model and control methods support the positioning accuracy of the antenna actuator.<sup>13</sup> Krejčí et al. (2012) provided evidence of the applicability of the arctangent function to approximate a hysteretic curve in the  $T(x)$  hysteresis mode.<sup>14</sup> Bieńkowski et al. (2023) later provided evidence of the ability of arctangent functions in the  $T(x)$  model to describe the nonlinear nature of hysteresis.<sup>15</sup> These findings confirm that arc-based functions are a reliable way to model hysteresis, and this is what is done in the present study of modeling experimental data with the arctangent function because it is continuous, finite and reversible.<sup>16</sup> This work provides an accurate model despite its simplicity and stability and has been experimentally verified, unlike previous studies based on dynamic models and complex data. Therefore, it can be adopted to improve control and practical implementation.

### Proposed Design

The pneumatic muscle actuator consists of a tiny air entrance, an inner tube, and a braided mesh in order to direct and limit the tube's deformation. It is closed on both sides Figure 1. The actuator's action is defined by the braiding angle ( $\theta$ ), with a critical value of  $54.7^\circ$ . Exhibits contraction behavior when it is below the critical value, but an extension behavior for the air muscle is produced by a greater braiding angle Figure 2.<sup>15-18</sup>

For manufacturing the artificial air muscle was using materials that were compatible with the design so that they were soft and simple. The process was done using a 34 cm long tube cover by a braided sleeve, with 25 cm less than the length of the tube was used (because the muscle is contraction type, the length braided sleeve must be as compressed as possible to make angle between the filaments of the braided sleeve and the longitudinal sheath of the muscle less than critical value) and 20 mm diameter, end caps manufactured from Teflon by a 3D printer with a diameter of 20 mm

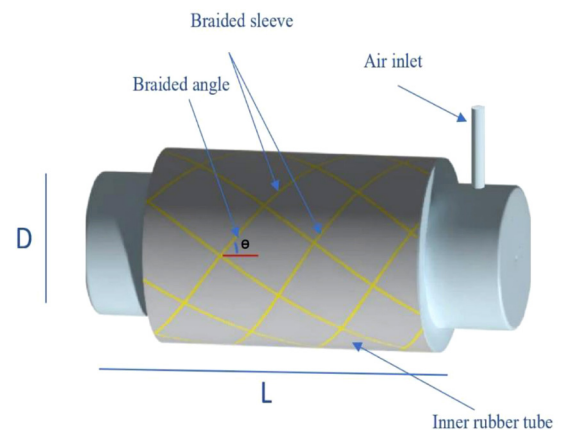


Fig 1 | The structure of the pneumatic muscle actuator

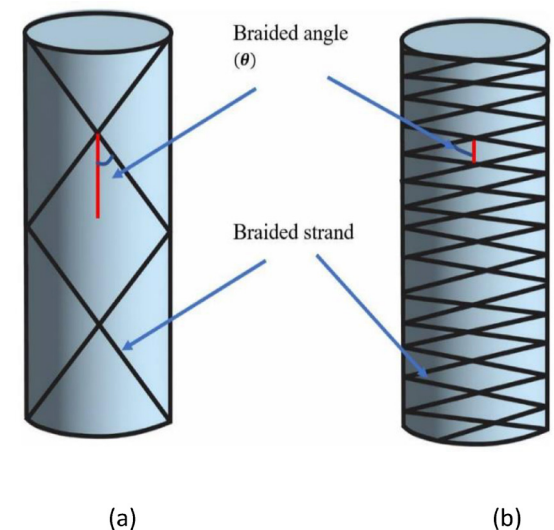


Fig 2 | The braided angle of PMA (a) Contraction actuator (b) Extension actuator

and a length of 35 mm, one of them containing an air inlet with a diameter of 5 mm to supply muscle by air. end caps were tightly inserted in the outskirts of tube then covered by braided sleeve, duct tape Cable tape was used to fixed the ends and braided sleeve for prevent leakage of air. The complete muscle have weight 70 grams with 30 cm length. All material and complete muscle shown in Figure 3.

For modeling the hysteresis phenomenon in pneumatic muscles to improve their performance and control accuracy. In this research, a mathematical model is developed to describe the hysteresis present in the pressure-length relationship in the muscle during the process of increasing and decreasing pressure. The arc tangent function was a Suitable choice to represent this nonlinear behavior as it is continuous, reversible, and finite. The model is expressed in a general form.<sup>16</sup>

$$y_{inc}(p) = a_0 \arctan(a_1 p + a_2) + a_3 \tag{1}$$

$$y_{dec}(p) = b_0 + \arctan(b_1 p + b_2) + b_3 \tag{2}$$

Where  $y_{inc}$  and  $y_{dec}$  are the lengths in cm when pressure increases and decreases respectively,  $p$  is the pressure in kPa,  $a_0$  and  $b_0$  expansion factor and Hysteria coefficient respectively both determine the height/depth of the arch (amount of hysteresis),  $a_1$  and  $b_1$  slope coefficient It controls the transition slope.,  $a_2$  and  $b_2$  Horizontal displacement, and  $a_3$  and  $b_3$  vertical displacement. To determine the coefficients that describe this function and as the relationship between pressure and length is non-linear, an algorithm called Nonlinear least squares curve fitting (lsqcurvefit) was suitable

for use to minimize the sum of squared errors between the model and the experimental values. The results showed that the model provides a high agreement with the data, so (1) and (2) became as follows:

$$y_{inc}(p) = 2.7378 \arctan(-0.0083212 p + 1.3402) + 27.759 \tag{3}$$

$$y_{dec}(p) = 2.7854 \arctan(-0.0088259 p + 1.1891) + 27.87 \tag{4}$$

The loading and unloading phase estimated parameters of the arctangent hysteresis model, along with their associated 95% confidence limits, are summarized in Table 1.

**Experimental Results**

This experiment aims to study the relationship between the air pressure pumped to the artificial pneumatic muscle and its length at a temperature of laboratory (20 to 30). Materials and tools used in the experimental setup as in the following:

- a. Artificial pneumatic muscle 30 cm long.
- b. Air pressure regulator to adjust the pressure level.
- c. Air pump to provide air.
- d. Pressure sensor to measure the applied pressure.
- e. Distance sensor to measure change in length
- f. Arduino is a Mega for reading data generated by sensors.
- g. Jumper wires (male to male) to connect sensors to Arduino ports. All of the material and tools are shown in Figure 4 in the same order.



(a)



(b)



(c)



(d)

**Fig 3 | Material to manufacturing PMA (a) ends manufactured by a 3D printer (b) a 34 cm long tube (c) braided sleeve (d) photograph of PMA**

To demonstrate the behavior of the system, the artificial pneumatic muscle was suspended vertically in a frame, and its free end was equipped with a distance sensor to measure the change in its length (There may be errors in the sensor readings). As we know the distance sensor use to measure the distance between it and objects so to make it measure the length of muscle use a code in Arduino that gives in zero kPa 30 cm (length of muscle), to ensure that the reading is correct, the length was measured manually using a ruler after each increase in pressure. Then, the air pump was connected to a pressure sensor (There may be errors in the sensor readings). and then attached to the muscle, and an

Arduino was used to obtain the readings of the two sensors instantly. The pressure was increased from zero to 500 kPa in steps of 50 by valve (provides gauge pressure) that give Read the pressure on its own screen so can ensure that read of sensor is correct, cannot use above 500 kPa because the muscle may be damaged, air may leak, or it may burst and cause damage, and then the pressure was reduced at the same rate from 500 kPa to zero to determine the relationship towards return. The change in length was recorded at each step as the pressure increased and decreased the two operations were performed three times and the average was taken, and the result was as shown in Figure 5 and Table 2.

**Table 1 | Estimated parameters of the arctangent hysteresis model with 95% confidence intervals for loading and unloading**

Branch	Symbol	Estimate	95% CI (Low)	95% CI (High)
Up (Loading)	a0	2.737800	1.986400	3.489300
Up (Loading)	a1	-0.008321	-0.012396	-0.004247
Up (Loading)	a2	1.340200	0.503060	2.177300
Up (Loading)	a3	27.759000	27.261000	28.258000
Down (Unloading)	b0	2.785400	2.017600	3.553300
Down (Unloading)	b1	-0.008826	-0.012970	-0.004682
Down (Unloading)	b2	1.189100	0.402640	1.975500
Down (Unloading)	b3	27.870000	27.282000	28.458000

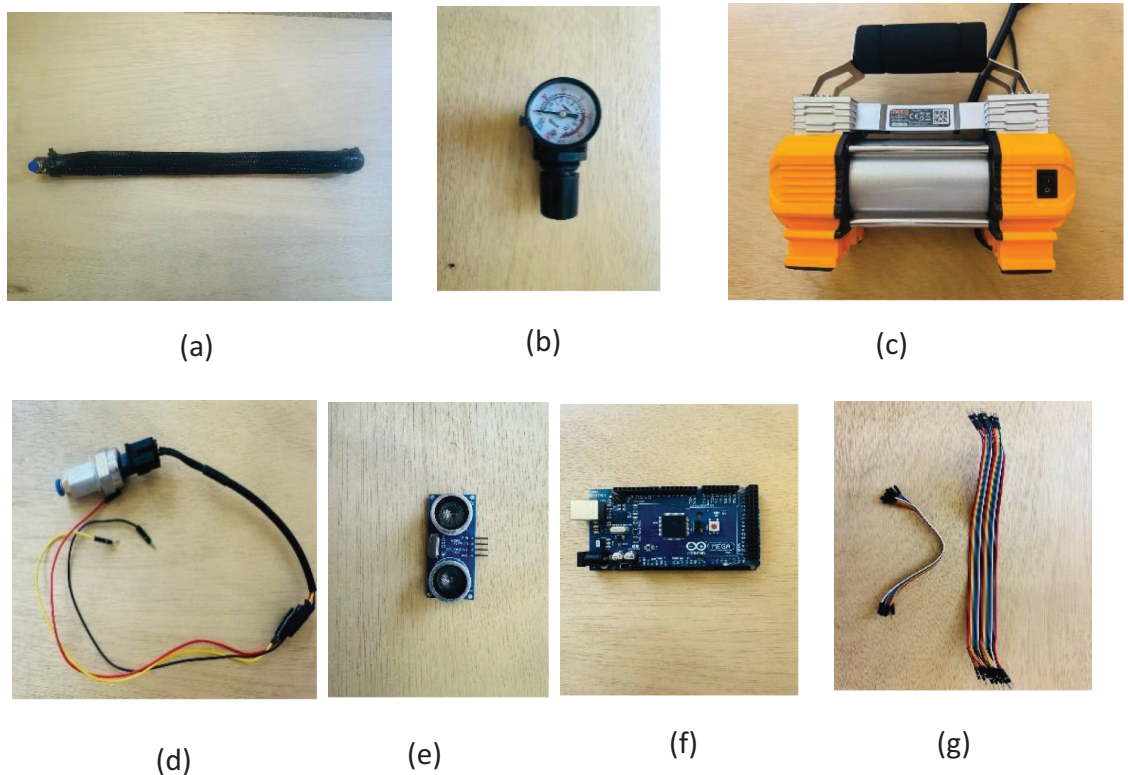


Fig 4 | Materials and tools used in the experimental setup

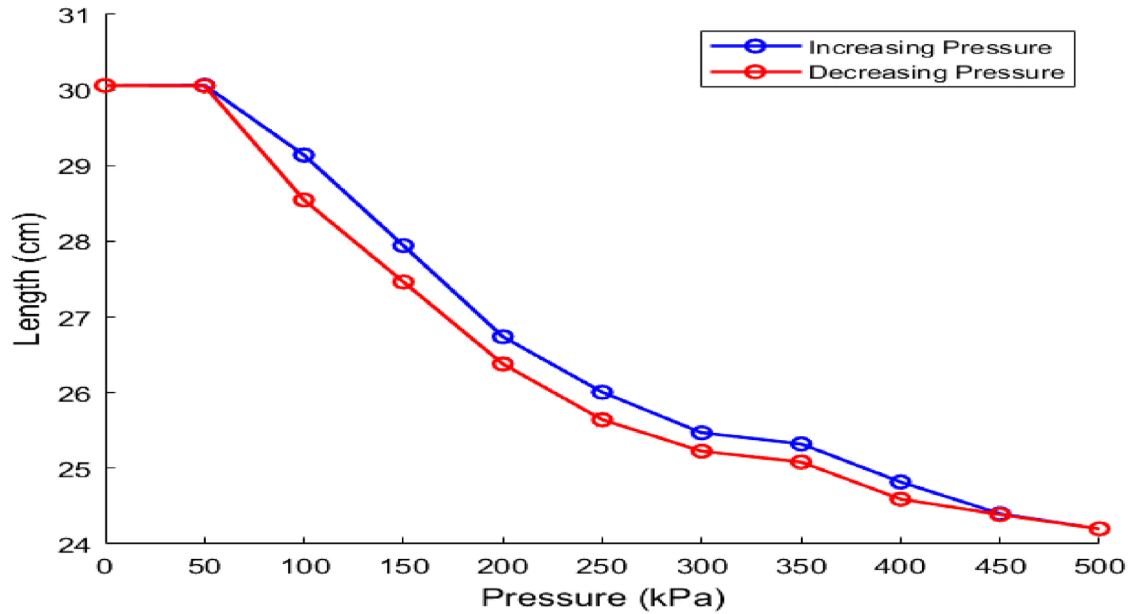


Fig 5 | Relationship between the length of the artificial pneumatic muscle and the pressure during loading and unloading stages

Pressure (kPa)	Up mean (cm)	Up SD (cm)	Up CI (cm)	Down Mean (cm)	Down SD (cm)	Down CI (cm)
0	30.053	0.047	0.117	30.05	0.046	0.114
50	29.72	0.624	1.549	30.073	0.015	0.038
100	29.14	0.266	0.662	28.853	0.301	0.748
150	27.943	0.414	1.029	27.51	0.259	0.643
200	26.527	0.055	0.137	26.307	0.127	0.316
250	25.64	0.167	0.415	25.7	0.104	0.258
300	25.47	0.053	0.131	25.323	0.162	0.402
350	25.323	0.153	0.379	25.217	0.237	0.588
400	24.82	0.164	0.407	24.713	0.214	0.531
450	24.4	0.115	0.287	24.38	0.017	0.043
500	24.2	0.095	0.237	24.197	0.006	0.014

Figure above shows the relationship between the length of the artificial pneumatic muscle and the pressure. The blue curve shows a decrease in length when the pressure increases and the red curve shows an increase in length when the pressure decreases. Reasons for the length to remain constant between zero and 50 kPa. There is no friction between the braid and the tube and the resistance of the tube, while the reason for its stability between 450 kPa and 500 kPa is that at a certain pressure, the material from which the muscle is made reaches saturation and cannot be compressed or stretched. Also observed is a difference in the length values in the two stages at the same pressure. This is attributed to irregular characteristics. The structure of the complicated behavior of the PMA outer coating, the com-

pressibility of air, and the elastic-viscous attributes of the inner rubber tube all contribute to this nonlinearity. Not to mention the hysteresis because of the inner rubber tube, so the PMA's performance varies under various pressurizing situations, causing the system to become more complicated as a result of this behavior<sup>19</sup> in addition the Table 1 indicates the accuracy of the experimental setup due to the low standard deviation values, CI values also indicate that the data are reliable and the measurement process is accurate.

The validity of this model was confirmed by comparing the simulated values resulting from the appropriate arc tangent function with the experimental data. Statistical evaluation measures such as the mean square error and the coefficient of determination were used to

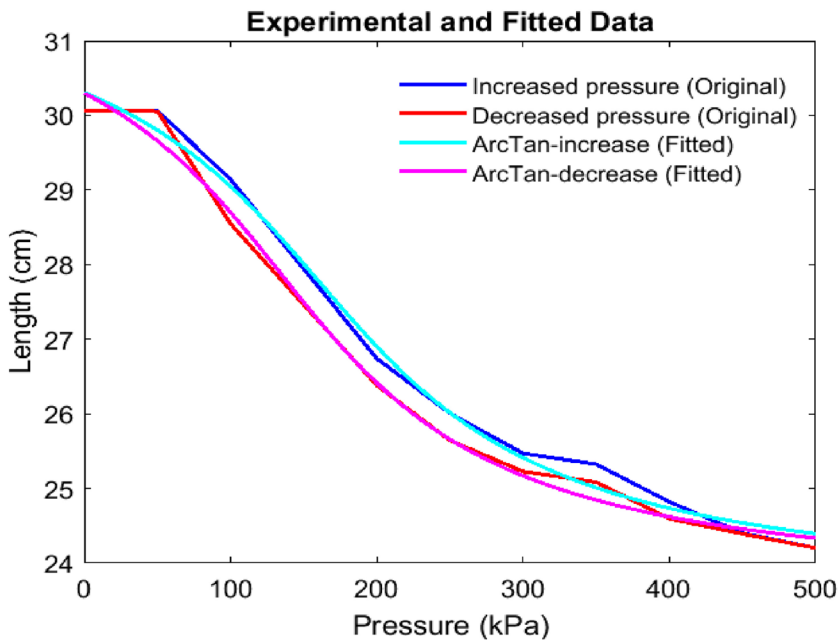


Fig 6 | Visual comparison between simulation from arc tangent values and experimental values

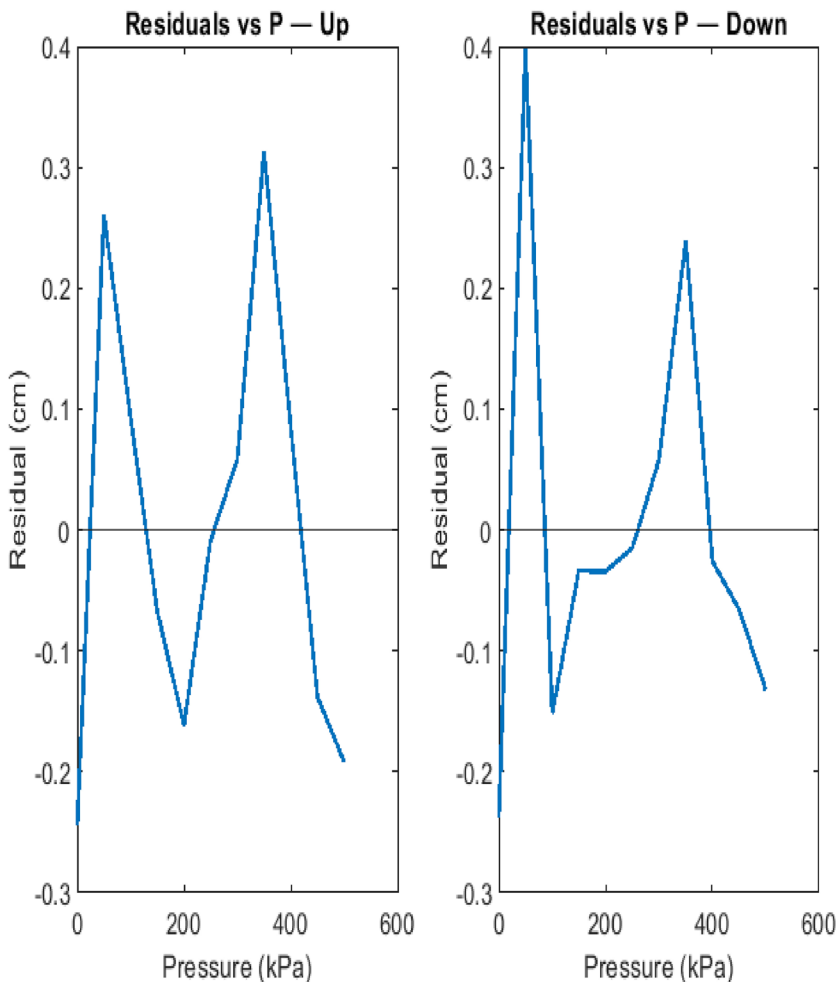


Fig 7 | Residual curves

determine the accuracy of the model. In the ascending stage, the MSE was at a value (0.030238), small value of MSE means that the model is more accurate in predicting the data.  $R^2$  is at a value (0.99322) RMSE is at value (0.17389) and MAE at (0.14769), which means a strong agreement between the simulated and experimental values. Likewise, in the descending stage, where the MSE was at a value (0.029424),  $R^2$  is at a value (0.99328) RMSE at value (0.17153) and MAE (0.12645), which confirms the validity of the model. In addition to this visual comparison through the graphs, it shows a close agreement between the simulated and experimental data, as shown in Figure 6, a clear convergence between the experimental and calculated data, that enhances the strength of the model and residual curve in Figure 7 for loading and unloading phases.

This Figure clear the residuals are randomly distributed around zero with small amplitudes ( $\pm 0.3$  cm), which indicates that the model errors are random and do not have systematic bias. This confirms that the arctangent model is adequate in representing the pressure–length relation and the hysteresis property of the pneumatic artificial muscle.

**Calibration of Sensors**

**Sensor of Pressure**

A steel analog pressure sensor with a range of (0–0.5) MPa (0–500) kPa. According to the datasheet from the manufacturer Robu (2025),<sup>20</sup> this sensor provides a linear output from 0.5 V at 0 kPa to 4.5 V at 500 kPa when supplied with a 5 V voltage. Arduino Mega 2560 was programmed to covert the voltage to pressure in kPa by the following equation:

$$P_{kpa} = \frac{V_{out} - 0.5}{4.0} \times 500 \tag{5}$$

Where  $V_{out}$  is measured voltage, instantaneous pressure value in kPa is show live in serial monitor during experimental. the ADC resolution of the Arduino is approximately 0.61 kPa per step which it is very small (negligible) compared to sensor’s accuracy is  $\pm 2\%$  of full scale, corresponds to approximately  $\pm 10$  kPa, at 95% confidence level ( $k = 2$ ) approximately  $\pm 20$  kPa is the expanded uncertainty according to the datasheet Robu (2025).<sup>21</sup>

**Sensor of Distance**

According to the data sheet (SparkFun) (2025)<sup>19</sup> HC-SR04 sensor works by sending an ultrasonic pulse and receiving the reflected pulse from the other end of the muscle, this sensor used to measure the length of the muscle after contraction, the instantaneous length of the muscle is calculated using the equation:

$$L_{cm} = \frac{t_{\mu s}}{58} \tag{6}$$

Where  $t_{ms}$  is the pulse return in microseconds, An Arduino 2560 board was programmed to send a pulse of 10 microseconds from the TRIG pin and read the ECHO signal via the pulse In and convert it to a length in cm which is display in real time on serial monitor through experimental. The sensor range is (2 – 400) cm with an accuracy of approximately 3 mm, the measurement uncertainty increases by  $\pm 0.175\%$  of the measured distance per C° this because of effect of temperature on the speed of sound according to data sheet.<sup>22</sup>

**Comparasion arc Tangent Function Model with Bouc-wen Model**

On applying the Bouc–Wen model to the experimental data as shown in Figure 8, statistical analysis indicated higher precision with larger  $R^2$  ( $\approx 0.995$ ) and smaller error measures compared to the Arc tangent model as in Tables 3 and 4. However, the Bouc–Wen model is parameter demanding and complex calibration and therefore less desirable for real-time control application.<sup>23</sup> Conversely, the Arc tangent model, although slightly less accurate ( $R^2 \approx 0.993$ ), is mathematically simple, has fewer parameters, and is simpler to implement in control systems.<sup>24</sup> Therefore, in summary, Bouc–Wen is the more accurate model, but the Arc tangent function provides the more practical trade-off between accuracy and simplicity for real-time applications.

**Limitations and Future Work**

This research presents an analysis of the relationship between the supplied pressure and muscle length during pressure increase and decrease. Therefore, this work focuses on the static characterization of the artificial muscle without considering the dynamic effects and long-term material behavior. By optimizing the minimum loading experiments and advanced modeling to find the time- and rate-dependent behaviors, future work will be expanded for broader applications

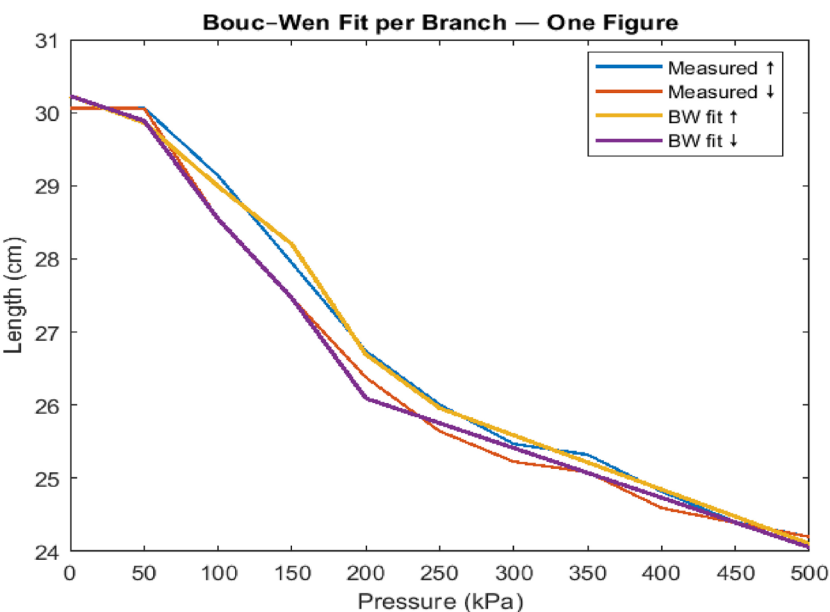


Fig 8 | Experimental data and Bouc-wen model

**Table 3 | Statistical evaluation in ascending stage**

The Statistical Evaluation Increase Stage	Arc Tangent Function	Bouc-wen Model
MSE	0.030238	0.025732
$R^2$	0.99322	0.994229
RMSE	0.17389	0.160412
MAE	0.14769	0.132812

**Table 4 | Statistical evaluation in descending stage**

The Statistical Evaluation Increase Stage	Arc Tangent Function	Bouc-wen Model
MSE	0.029424	0.020634
$R^2$	0.99328	0.995290
RMSE	0.17153	0.143645
MAE	0.12645	0.110927

**Conclusion**

In conclusion, the research presents a study of modeling the phenomenon of hysteresis in artificial pneumatic muscles using the arctangent function which characterized by the ease of mathematical representation and flexibility of modification based on experimental data, unlike the traditional models mentioned in previous studies. This makes it a suitable choice for modeling hysteresis. A practical model was reached that describes the relationship between pressure and length in artificial pneumatic muscles, taking into account the hysteresis that exists in this relationship. Based on the experimental data, the optimal parameters of the model were determined using the curve-fitting method in MATLAB. Statistical indicators such were used such as MSE, RMSE, MEA and  $R^2$  then comparison with statistical indicators to Bouc-wen model. The model was evaluated and showed a high agreement between the experimental and simulation values. The model demonstrated its ability to accurately represent hysteresis, which supports its use in improving the design and control of artificial pneumatic muscles so can use in control system of soft robotic, easy to implement and its experimental can do in laboratory. In this research, an important step was presented towards understanding and analyzing the nonlinear behavior in artificial aerobic muscles, which helps in developing applications for this technology in the field of soft robotics and intelligent systems.

**References**

- 1 Joe S, Totaro M, Wang H, Beccai L. Development of the ultralight hybrid pneumatic artificial muscle: Modelling and optimization. PloS one, 2021;16(4), e0250325.
- 2 Kalita B, Leonessa A, Dwivedy SK. A review on the development of pneumatic artificial muscle actuators: Force model and application. Actuators. 2022;11(10):288. <https://doi.org/10.3390/act11100288>

- 3 Xavier MS, Tawk CD, Zolfagharian A, Pinskiar J, Howard D, Young T, et al. Soft pneumatic actuators: A review of design, fabrication, modeling, sensing, control and applications. *IEEE Access*. 2022;10:59442–85. <https://doi.org/10.1109/ACCESS.2022.3179589>.
- 4 Abu Mohareb S, Alsharkawi A, Zgoul M. Hysteresis modeling of a PAM system using ANFIS. *Actuators*. 2021;10(11):280. <https://doi.org/10.3390/act10110280>.
- 5 Xie S, Ren G, Xiong J, Lu Y. A trajectory tracking control of a robot actuated with pneumatic artificial muscles based on hysteresis compensation. *IEEE Access*. 2020;8:80964–77. <https://doi.org/10.1109/ACCESS.2020.2991196>
- 6 Zhang X, Diao S, Yang T, Fang Y, Sun N. LSTM-NN-Enhanced Tracking Control for PAM-Driven Parallel Robot Systems with Guaranteed Performance. *IEEE Transactions on Circuits and Systems I: Regular Papers*. 2025. <https://doi.org/10.1109/TCSI.2024.3522885>
- 7 Shakiba S, Ourak M, Vander Poorten E, Ayati M, Yousefi-Koma A. Modeling and compensation of asymmetric rate-dependent hysteresis of a miniature pneumatic artificial muscle-based catheter. *Mechanical Systems and Signal Processing*. 2021;154:107532. <https://doi.org/10.1016/j.ymssp.2020.107532>
- 8 Xie S, Liu H, Wang Y. A method for the length-pressure hysteresis modeling of pneumatic artificial muscles. *Science China Technological Sciences*. 2020;63(5):829–37. <https://doi.org/10.1007/s11431-019-9554-y>
- 9 Ru H, Yang Y, Wang B, Huang J. Model predictive control for a bending pneumatic muscle based on an online modified generalized Prandtl-Ishlinskii model. *Neural Computing and Applications*. 2024;1–13. <https://doi.org/10.1007/s00521-024-09666-2>
- 10 Sheikh Sofla M, Sadigh MJ, Zareinejad M. Precise dynamic modeling of pneumatic muscle actuators with modified Bouw-Wen hysteresis model. *Proceedings of the Institution of Mechanical Engineers, Part E: Journal of Process Mechanical Engineering*. 2021;235(5):1449–57. <https://doi.org/10.1177/09544089211008000>
- 11 Ru H, Huang J, Chen W, Xiong C. Modeling and identification of rate-dependent and asymmetric hysteresis of soft bending pneumatic actuator based on evolutionary firefly algorithm. *Mechanism and Machine Theory*. 2023;181:105169. <https://doi.org/10.1016/j.mechmachtheory.2022.105169>
- 12 Ma G, Jia H, Xia D, Zhang Z, Hao L. Study of Hysteresis Modeling on the Pneumatic Muscle Humanoid Elbow Joint. In: 2024 36th Chinese Control and Decision Conference (CCDC). IEEE; 2024. p. 604–9. <https://doi.org/10.1109/CCDC62350.2024.10587710>
- 13 Zhang Y, Qi H, Cheng Q, Li Z, Hao L. Modeling and Compensation of Stiffness-Dependent Hysteresis Coupling Behavior for Parallel Pneumatic Artificial Muscle-Driven Soft Manipulator. *Applied Sciences*. 2024;14(22):10240. <https://doi.org/10.3390/app142210240>
- 14 Takács, J. Mathematics of hysteretic phenomena: the T(x) model for the description of hysteresis. 2003, (p. 173).
- 15 Chwastek KR, Jabłoński P, Kusiak D, Szczegielniak T, Kotlan V, Karban P. The effective field in the T(x) hysteresis model. *Energies*. 2023;16(5):2237.
- 16 Xie S, Ren G, Wang B. A modified asymmetric generalized Prandtl-Ishlinskii model for characterizing the irregular asymmetric hysteresis of self-made pneumatic muscle actuators. *Mechanism and Machine Theory* 2020;149:103836.
- 17 Elsamanty M, Hassaan MA, Orban M, Guo K, Yang H, Abdrabbo S, et al. Soft Pneumatic Muscles: Revolutionizing Human Assistive Devices with Geometric Design and Intelligent Control. *Micromachines*. 2023;14(7):1431.
- 18 Al-Ibadi A, Nefti-Meziani S, Davis S. The design, kinematics and torque analysis of the self-bending soft contraction actuator. In: *Actuators*, vol. 9, no. 2. Basel (Switzerland): MDPI; 2020 Apr. p. 33.
- 19 Al-Mosawi HA, Al-Ibadi A, Abdalla TY. A comprehensive comparison of different control strategies to adjust the length of the soft contractor pneumatic muscle actuator. *Iraqi J Electr Electron Eng*, 2022;18(2):101–109.
- 20 Abed AA, Al-Ibadi A, Abed IA. Vision-based soft mobile robot inspired by silkworm body and movement behavior. *J Robot Control*. 2023;4(3):299–307.
- 21 Robu. 0.5 MPa Stainless Steel Pressure Transducer Sensor. Robu. [Online]. 2025, Available: <https://robu.in/product/0-5mpa-stainless-steel-pressure-transducer-sensor/> [Accessed: 29-Aug-2025].
- 22 SparkFun, "HC-SR04 Ultrasonic Ranging Module," Datasheet. [Online]. Available: <https://cdn.sparkfun.com/datasheets/Sensors/Proximity/HCSR04.pdf>. [Accessed: 29-Aug-2025].
- 23 Ikhouane F, Rodellar J. On the hysteretic Bouc–Wen model: Part I: Forced limit cycle characterization. *Nonlinear dynamics*, 2005;42(1):63–78.
- 24 Perez-Rojas C. Fitting saturation and hysteresis via arctangent functions. *IEEE Power Engineering Review*, 2005;20(11):55–57.